NÖHÜ Müh. Bilim. Derg. / NOHU J. Eng. Sci., 2023; 12(4), 1219-1231

Niğde Ömer Halisdemir Üniversitesi Mühendislik Bilimleri Dergisi
Niğde Ömer Halisdemir University Journal of Engineering Sciences

Araştırma makalesi / Research article

www.dergipark.org.tr/tr/pub/ngumuh / www.dergipark.org.tr/en/pub/ngumuh

Assessment of UV-vis driven CFT-GO based photocatalysis on the conjugative gene transfer mechanism in a pilot plant system

UV-VIS kaynaklı CFT-GO tabanlı pilot ölçek fotokataliz prosesinin konjugatif gen transfer mekanizmasına etkisinin belirlenmesi

Can Burak Özkal[1,*]

[1] *Tekirdağ Namık Kemal Üniversitesi, Çevre Mühendisliği Bölümü, 59860, Tekirdağ Türkiye*

Abstract

This study addresses the need for sustainable methodologies in antimicrobial resistance (AMR) surveillance, particularly in wastewater treatment, to ensure efficient disinfection and control of AMR. The use of photocatalysis (PC) has gained attention as a scalable and suitable approach for research and development. This study evaluates the effect of UV-vis driven sub-lethal photocatalytic oxidation on conjugative gene transfer between two E. coli strains using a pilot plant reactor system. Photocatalysts composed of graphene-oxide-Ti-CuFe2O4 nanocomposites were synthesized through a green approach and used to enhance bacteria inactivation rates, resulting in hindered frequency and absolute abundance of trans-conjugants in the recipient strains. Experiments plan was built with the intent to determine the contribution of photocatalyst type, mode of operation on the conjugation mechanism and also distinguish between the scenarios where individual or simultaneous exposure to PC oxidation of donor and recipient strains occur. Simultaneous photocatalytic treatment of both donor and recipient strains resulted in the removal of ~3 LOG of both bacteria and eligible conditions were obtained for controlling trans-conjugants formation compared to no treatment conditions. The photocatalyst surface, reactive oxygen species, and bacterial cells' interaction played a determining role in controlling ARG transfer. The impact of photocatalytic oxidation mechanisms on the vitality of recipient cells was evident during the continuous mode of operation, where conjugative transfer of ARGs was mitigated, and the number of trans-conjugants decreased to below 102 CFU mL-1. This study demonstrates the potential of PC for efficient disinfection and control of AMR in wastewater treatment.

Keywords: Antibiotic resistance, Antibiotic resistance gene, Conjugative gene transfer, Photocatalysis, Bacteria inactivation

Öz

Bu çalışma, antimikrobiyal direncin kontrolünde (AMR) sürdürülebilir yaklaşımlar arasında olan, atıksuyun etkin dezenfeksiyonu üzerine kurulmuştur. Fotokataliz prosesi, ölçeklenebilir, araştırma ve geliştirmeye açık bir ileri oksidasyon prosesidir. Deneysel çalışmalarda kullanılan grafen-oksit-Ti-CuFe2O4 nanokompozit fotokatalizörleri, yeşil bir yaklaşımla sentezlenmiştir. Parabolik kolektör destekli fotoreaktörde, sub-letal fotokatalitik oksidasyonun alıcı ve verici E. coli suşları arasındaki konjugatif gen transferi mekanizmasına etkileri deneysel olarak araştırılmıştır. Farklı fotokatalizörlerin bakteri inaktivasyon hızı üzerine etkisi yanında, alıcı suşlarda eşleşmiş çiftlerin oluşumu (transkonjugan) frekansını ve nihai miktarını azaltan bir etki gösterdiği ortaa konulmuştur. Deney planı, fotokatalizör tipinin ve proses işletme modunun konjugasyon ile gen tranfer mekanizmasına katkısını belirlemek, verici ve alıcı suşların PC oksidasyona tekil veya eşzamanlı maruz kalma senaryoları arasındaki farkı ortaya koabilmek amacıyla oluşturulmuştur. Alıcı ve verici suşların eşzamanlı olarak fotokatalitik oksidasyona maruz kalması, her iki suş için de yaklaşık ~3 LOG giderim sağlamış ve transkonjugan oluşumunu kontrol edebilecek koşular oluşturmuştur. Fotokatalizör yüzeyi, reaktif oksijen türleri ve bakteriyel hücrelerin etkileşimi, ARG transferinin kontrolünde belirleyici bir rol oynamıştır. Alıcı hücrelerin canlılığı üzerindeki fotokatalitik oksidasyon mekanizmalarının etkisi, konjugatif ARG transferinin azaltıldığı sürekli işletme sırasında açıkça görülmüş ve transkonjuganların sayısı 102 CFU mL-1'nin altına düşmüştür. Bu çalışma, PC'nin atıksu arıtımında etkili dezenfeksiyon ve AMR kontrolü için potansiyelini göstermektedir.

Anahtar kelimeler: Antibiyotik direnci, Antibiyotik direnç geni, Konjugatif gen transferi, Fotokataliz, Bakteri inaktivasyonu

1 Introduction

The misuse, overuse, and inadequate disposal of antibiotics have resulted in a significant increase in antibiotic resistance genes (ARGs). Antibiotics exert selective pressure on bacteria, and ARGs emerges as a response and the need for the development of new antibiotics arises [1–3].

Specific measures can be taken at waste water treatment plants (WWTP) and industrial discharge rates to mitigate the AMR and ARG associated risks [4–6]. ARGs are DNA

* Sorumlu yazar / Corresponding author, e-posta / e-mail: cbozkal@nku.edu.tr (C. B. Özkal)
Geliş / Recieved: 19.04.2023 Kabul / Accepted: 07.09.2023 Yayımlanma / Published: 15.10.2023
doi: 10.28948/ngumuh.1285885

fragments that encode antibiotic resistance. They are present in mobile genetic elements, chromosomal and extrachromosomal DNA, while the latter possess persistency and transformation abilities. Plasmids, transposons, and integrons are mobile genetic elements that have high transfer capacities and facilitate the horizontal transfer of resistance genes between bacterial species and strains. HGT occurs through four mechanisms; conjugation, transformation, transduction, and gene transfer agents. Even after bacterial cell death, ARGs can persist in the environment as genetic material for extended periods, which can be acquired by other bacteria through the transformation mechanism [7–9].

It was hypothesized in the last decade that wastewater treatment plant (WWTP) effluents may act as a source and carrier of mobile genetic elements into downstream environments. Therefore, it is essential to prioritize the development and dissemination of wastewater treatment (WWT) alternatives that can achieve AR control [10,11]. The proliferation of multidrug-resistant bacteria is attributed to an increase in transconjugant numbers [12]. Given the global nature of the antibiotic resistance crisis, not only changes in conjugative transfer frequencies but also the abundance and fate of transconjugants in a unit volume of treated water must be monitored. Treatment process mechanisms play a crucial role in the level of bacterial inactivation, HGT inhibition, reduction, and inhibition of bacterial reactivation [13–15].

Recent studies have highlighted the significant impact of advanced oxidation processes on HGT mechanisms. NaClO has been found to enhance cell permeability [16], while nano Al_2O_3 has been shown to promote expression mating pair formation between *E. coli* species (via RP4 plasmid) due to oxidative stress. Additionally, "sub-lethal photocatalysis" with nano ZnO and nano TiO_2 has resulted in increased cell permeability and over 20- and 70-fold increases in the CGT, respectively. Meanwhile, CuO, Ag, and Fe_2O_3 in nano form have been reported to cause approximately a two-fold increase in HGT [17–19]. The bacterial defense mechanisms against reactive oxygen species (ROS)-induced cellular damage may play a decisive role in total and antibiotic-resistant bacteria species. The DNA damage resulting from UV-based disinfection processes, including UV/H_2O_2 and UV/chlorination, remains tolerable due to the substantial effect of $\dot{O}H$ on DNA structure and depletion by intracellular components [20]. Disinfectants such as chlorine and hypochlorous acid have also been found to promote the conjugative transfer of ARGs. However, chlorination at high doses has been reported to cause changes in cell membranes [3,16,21].

In the practical application of photocatalytic technology for wastewater treatment, variations in water quality may lead to bacteria cells to survive ROS-induced stress [22,23]. Besides, sub-lethal photocatalysis has the potential to increase intracellular ROS levels in ARB and activate antioxidant systems. These mechanisms are known to trigger the HGT of ARGs through transformation and conjugative transfer mechanisms. The mode of process operation and photocatalyst choice play a determining role in the mechanism of conjugative transfer in the treated effluent [24–26].

The photocatalytic process is currently transitioning from laboratory-scale to pilot and full-scale applications, thanks to recent advances in the field of photocatalyst synthesis and reactor design. This can be achieved through doping semiconductor photocatalysts with metal dopants, forming heterojunctions between semiconductors, band gap narrowing, impurity energy level reduction, and the creation of oxygen vacancies [27]. Graphene-based composite structures and spinel ferrite-based nanocomposites are widely used in photocatalysis and adsorption processes for pollutant removal. However, graphene oxide (GO) and reduced GO may cause intracellular ROS accumulation, affecting bacterial cell membrane structure and hindering the conjugative transfer of RP4 plasmid-borne ARGs. The membrane stability also plays a significant role in HGT, where graphene oxide/reduced graphene oxide sheets can damage the cell membrane and contribute to the conjugative transfer mechanism [28-32]. Additionally, for disinfection using graphene-based TiO_2 nanocomposites, the adhesive interaction between the photocatalyst and bacteria is a crucial factor in achieving total inactivation and preventing re-growth mechanisms [33-36].

Recent studies have investigated the potential contribution of environmental photocatalyst interfaces in the co-existence of natural minerals and light irradiation [37]. To understand bacterial responses to transformed nanomaterials, researchers have examined the effect of naturally occurring photocatalysts on horizontal gene transfer (HGT) mechanisms of antibiotic-resistant (AR) bacteria, with a particular focus on sphalerite applications. The study by Yin in 2021 found that UV-A and UV-vis-based photocatalysis using sphalerite increased HGT by 2-10 and 1-2 folds, respectively [33,38].

As natural water matrices contain graphene oxide (GO) that may undergo different reduction processes, resulting in significant variations in ARG propagation mechanisms by conjugation [39], this study aims to determine the effect of photocatalytic oxidation at sub-lethal process conditions on the conjugative gene transfer mechanism between two *E. coli* strains (DSM-3876 donor and ATCC33694 recipient). Experiments were carried out in a pilot plant photocatalysis reactor at continuous and batch modes of operation. Effects of photocatalytic oxidation on the rate of conjugative gene transfer have been determined for GO based photocatalysis under UV-vis irradiation in comparison with the UV-A driven TiO_2 based photocatalysis.

2 Materials and methods

2.1 Bacterial strains and growth procedures

The experimental study utilized two strains of *E. coli*, namely Streptomycin resistant ATCC 33694 and Ampicillin, Tetracycline, and Kanamycin resistant J-53 (3876), which represent facultative pathogenic bacterial groups. The *E. coli* J-53 (DSM-3876) strain, which harbors the RP4 plasmid, was used as the donor, while the *E. coli* ATCC 33694 strain, which confers plasmid resistance to Streptomycin antibiotic, was selected as the recipient strain. The main objective of the

study was to investigate the effect of sub-lethal PC process on the frequency and occurrence of conjugative ARG transfer, as well as to confirm that resistance gene transfer from donor to recipient strains can be achieved via plasmid RP4 [40,41].

Initially, single colonies of both bacterial strains were taken from refrigerated stock plates and cultured in Luria-Bertani liquid broth, supplemented with ampicillin (100 µg/mL), kanamycin (50 µg/mL), tetracycline (16 µg/mL), and streptomycin (200 µg/mL) [23,42].

The cultures were then incubated at 37 °C for 20 hours, and 100 µL of cells were streaked onto agar plates containing the corresponding antibiotic concentrations. The antibiotic resistance behavior of both strains was initially validated using agar dilution methodology, based on their growth ability on the corresponding agar plates. The initial bacterial concentration was determined by measuring the absorbance at 600 nm wavelength using McFarland standards with 0.8% NaCl.

The successfully mated strains, which gained multiple resistance to both Amp, Kan, Tet, and Str antibiotics via conjugative transfer of ARGs, were isolated and stored in glycerol stock solution at -80 ^{0}C for further experiments.

2.1.1 Chemicals

The experimental setup also involved the use of $CuCl_2$, $FeCl_3$, NaOH, citric-acid in powder form, PEG 600 (CAS #25322-68-3), titanium dioxide (TiO_2: CAS# 1317-70-0), and titanium tetra-Isopropoxide solution (CAS#546-68) to achieve desired chemical reactions. Additionally, a graphene oxide solution was prepared by diluting a GO flake suspension (4 mg mL^{-1} suspension; Sigma-Aldrich) with distilled water to attain a final concentration of 2.5 mg mL^{-1}. The microbiological studies also utilized antibiotic standards such as Ampicillin sodium salt, Ampicillin (CAS 69-52-3), Streptomycin (CAS number: 3810-74-0), Tetracycline (CAS 64-75-5), and Kanamycin with analytical and cell culture grade purity.

2.1.2 Synthesis of photocatalysts

In this study, the nanocomposite synthesis procedure involved the use of Cydonia oblonga seed extracts (COSE) that were prepared as described in detail elsewhere [43]. The CFT-GO photocatalyst, which features a heterojunction with Schottky-like formation, was utilized due to its excellent UV-vis bacteria inactivation capabilities, as well as its characterization findings from a prior study [44]. The magnetically recoverable CFT-GO 3% (w/w) photocatalyst, which was synthesized via a combination of hydrothermal methods and sol-gel techniques in three consecutive steps, was chosen for experimentation based on its demonstrated superior bacterial inactivation potential in a recent study conducted by our research group [44].

The hydrothermal synthesis process was utilized to create the nanocomposite using COSE and a $CuCl_2$/$FeCl_3$ solution with a 1:2 mmol ratio. The resulting precipitate underwent washing, centrifugation, heating, and calcination steps as previously described [44]. A GO solution was prepared by diluting a GO flake suspension (4 mg mL^{-1}; Sigma-Aldrich) in distilled water to achieve the desired concentration. The GO/$CuFe_2O_4$ composite with the intended gravimetric ratio was generated following previously described procedures. The produced $CuFe_2O_4$-GO composite was subsequently added to the polymeric precursor solution. To produce the $CuFe_2O_4$-Ti-GO solution, the final product GO/$CuFe_2O_4$ was added to the polymeric precursor solution. The $CuFe_2O_4$-GO to Ti weight ratio was set to 3. The Ti(IV) polymeric precursor was created by maintaining constant 1:1:2 (w/w) ratios for Ti-isopropoxide, citric acid, and PEG. The Ti-isopropoxide-citric acid solution was prepared in distilled water while being continuously stirred for 18 h. PEG was then added under stirring conditions at 50 °C for 1 h.

2.1.3 Characterization of NC photocatalysts

The nanocomposite material was characterized using various analytical techniques. Scanning electron microscopy (SEM) was performed with magnification ranging from ×1000 to ×10,000, and energy dispersive X-ray analyses (EDX) were conducted using an FEI Quanta FEG250 instrument from Thermo-Fisher Scientific, Waltham, MA, USA. Fourier transform infrared spectroscopy analysis was conducted using a Vertex 70 model instrument from Bruker, Billerica, MA, USA. Raman spectroscopy was carried out at 532 nm excitation using a DXR instrument from Thermo-Fisher Scientific, and the analysis was performed at TNKU Central laboratory (NABİLTEM). In addition, diffuse reflectance, photo-luminescence, BET and XRD evaluations were performed, and detailed characterization and analysis parameter values have been provided in previous work [44].

2.1.4 Reactor configuration

To create a reactor system capable of operating under both solar and simulated UV irradiation, a pilot plant system was utilized. This system includes a concentrating parabolic collector composed of anodized aluminum parts, chosen for their high UV irradiation reflectance rates. This configuration enables the efficient collection and concentration of UV irradiation on the back side of the cylindrical photocatalysis reactor. The reactor itself is constructed from Plexiglass material due to its high UV transmission rate of >90%. The liquid is fed into the system using a sprinkler-like apparatus located at the top of the reactor, which sprays the liquid onto the inner surface of the reactor. During the heterogeneous photocatalysis process, the liquid flows down through the inner wall of the reactor via gravity and exits the system through a pneumatic valve before returning to the feeding tank. These details were reported in previous studies [45–50].

In order to enable the operation of a reactor configuration under both simulated UV and solar irradiation, a pilot plant system was designed and equipped with a concentrating parabolic collector, which is made of anodized aluminum parts due to their high UV irradiation reflectance rates. This configuration allows for efficient collection and concentration of UV irradiation on the back side of the cylindrical photocatalysis reactor, which is made of Plexiglass material, since it has a high UV transmission rate of over 90%. To initiate the heterogeneous photocatalysis process, a sprinkler-like apparatus placed on top of the reactor sprays the liquid onto the inner surface of the

cylindrical reactor, where gravity flow transports it down through the inner wall and out of the system via a pneumatic valve that leads back to the feeding tank. The UV irradiation is provided by Sylvana UV-visible and Philips UV-A fluorescent lamps, which are arranged parallel to the horizontal axis with a gap of 5 centimeters between them. The UV incident photon flux is maintained at around its solar equivalent level, with the average energy levels of UV-A and UV-visible light being 3.52 eV and 2.43 eV, respectively, as per the Planck constant h equivalent light necessary for photoexcitation. Accordingly, the UV-A and UV-visible irradiation levels are set at 2.20 and 3.30 mw cm^{-2}, respectively (measured by universal UV radiometer). The distance between the UV light and the plexi-glass reactor is 32 cm, and the back side of the plexi-glass reactor is subject to an average UV-A irradiation of 1.95 and an average UV-visible irradiation of 2.80 mw cm^{-2} (based on the average value of measurements made at 5 different vertical points). The total irradiated wet surface area of the plexi-glass reactor is calculated to be approximately 0.24 m^2. The system is capable of providing a flow rate of 60 L/hour and can be operated in two modes: continuous recirculating flow with internal surface spraying and simultaneous discharge or batch mode, where the inner surface of the cylindrical plexi-glass reactor is filled by spraying and then completely discharged. Considering the cylindrical surface area of the reactor, the velocity of flow is calculated to be 0.05 m s^{-1}, which is less than the average velocity of a stagnant stream flow, assumed to be 0.4 m s^{-1}.

Figure 1. Pilot plant photocatalysis reactor

In the batch mode of operation, the cylindrical reactor is filled up to 90% of its capacity and the liquid is allowed to flow out of the hole at the bottom of the tube under the force of gravity. The flow rates of feeding and discharging are nearly equal.

2.1.5 Ensuring sterile conditions

Before each experimental trial, the entire pilot plant system, including the photoreactor in contact with the liquid, was subjected to a sterilization process using a 70% ethyl alcohol solution, which was circulated within the system for 20 minutes duration. Subsequently, the photoreactor was rinsed with distilled water and left to dry under sunlight conditions. Microbial growth during the sterilization and drying cycle of the system was evaluated through periodic microbial contamination tests conducted during the experimental studies.

2.1.6 Determination of the sub-lethal photocatalysis conditions and bacteria inactivation levels

To investigate the effects of sub-lethal photocatalysis on bacterial activity, donor and recipient bacterial strains were diluted in 0.8% NaCl solution to their initial concentrations of 3.0-5.5 × 10^8 colony-forming unit (CFU) mL^{-1} and added to a 20 L feeding tank [23,38]. The photocatalysis process was conducted with minimal amounts of photocatalyst and reactive oxygen species (ROS), but for a sufficient duration to observe the effects of oxidative stress on bacterial cells and ARG transfer mechanisms (180 minutes). During the optimization phase, process parameters were adjusted, and the photocatalyst dose was set between 0.100 to 0.800 g L^{-1}.

In order to evaluate bacterial viability following photocatalytic treatment, liquid bacterial samples were obtained, and agar dilution and streak plate methodologies were employed. Each sample was streaked on three types of selective agar plates containing corresponding antibiotics including i) (200 µg/mL) streptomycin containing agar plates for counting St R^+ ATCC 33694 strain, ii) ampicillin (100 µg/mL), kanamycin (50 µg/mL), tetracycline (16 µg/mL) containing agar plates for counting Kan R^+, Amp R^+, Tet R^+ *E. coli* J-53 (DSM-3876) strain and iii) agar plates containing both ampicillin (100 µg/mL), kanamycin (50 µg/mL), tetracycline (16 µg/mL) plus (200 µg/mL) streptomycin antibiotics for counting the Kan R^+, Amp R^+, Tet R^+, St R^+ multi resistant strain. This way the donor, recipient, and conjugated strains could be counted separately [45,46]. The bacterial culture technique and serial dilutions of the reaction solution were prepared using a sterile 0.8% (w/w%) NaCl aqueous solution. The bacterial culture technique was performed in triplicate, and the minimum detectable colony number was approximately 2–3 CFU mL^{-1}. After incubation at 37 °C for 20–24 h, bacterial viable counts were determined by enumerating the colonies.

2.1.7 Assessment of ARG transfer frequencies

The primary objective of this study was to experimentally verify the transfer of resistance genes from a donor strain to a recipient strain through plasmid RP4 [40,41]. To compare and evaluate the occurrence and frequency of conjugative

antibiotic resistance gene transfer, the following experimental scenarios were investigated;
I) individual donor or recipient strains treated with photocatalysis (PC) and then mated with the untreated strain, and
II) samples collected during simultaneous exposure of both strains to PC treatment. To enable comparative evaluation, reference studies were replicated under UV-A, UV-vis only, and photocatalyst only conditions [42,47].

Considering the conjugative gene transfer; for *E.coli* the donor: recipient ratio was not found to play a decisive role in conjugative transfer frequency while conjugative transfer frequencies did not exhibit significant alterations when the initial bacteria concentrations > 10^5 CFU mL^{-1} [22]. The donor: recipient ratio parameter was set as 1:1, and initial bacterial concentrations as 10^8 CFU mL^{-1} keeping values at comparable levels to that referenced from recent literature findings [23,38][48]. The mating duration has been set between 4-24 hours during optimization studies.

Studies were carried out based on the pre-determined sub-lethal process conditions that may provide reproducible bacteria inactivation kinetics (as can be seen in Figure 4). The initial bacteria concentration was set as 1.2-2.5 10^8 CFU mL^{-1}. Individual bacterial cell suspensions are taken from the feeding tank as a function of the PC process duration and subjected to the conjugative gene transfer assessment (the mating protocol). 1 mL samples were added to the 9 mL Luria Bertani broth keeping volumetric donor/recipient ratio as 1:1, and incubated for 20 hours at 37 ^{0}C conditions. Prior to serial dilution, 100 uL aliquots were plated on Luria Bertani agars (as triplicates) containing related antibiotics. Recipients were determined by streaking onto LB plates with 200 ug L^{-1} streptomycin. Conjugants were determined by streaking onto LB plates with 100 ug L^{-1} ampicillin, 50 ug L^{-1} kanamycin, 16 ug L^{-1} tetracycline and 200 ug L^{-1} streptomycin [23,42,45,46].

Bacteria suspension of both donor and recipient strains at pre-set initial concentration were gently circulated within the reactor in the absence of photocatalyst, representative of the reference conditions. The enumeration results were used in the calculation of average colony counts (CFU mL^{-1}) from duplicate plates. Differences in colony counts across replicate experiments remained below %8. The limit of detection for the plating assay was 10 CFU mL^{-1}. The effect of each individual strain exposure to PC treatment (donor or strain) on conjugative gene transfer has been determined based on the frequency of conjugative transfer value that was calculated as = number of transconjugants (CFU mL^{-1}) / number of recipient cells (CFU mL^{-1}) [38,39].

2.1.8 Experimental

The experimental design consisted of several steps: firstly, sub-lethal photocatalytic (PC) conditions were determined by optimizing the PC dose and process duration based on the rate of bacteria inactivation [2,38]. The photocatalyst nanoparticles/nanocomposites were then added to a bacterial suspension with an initial concentration of 1.2-2.5 x 10^8 CFU mL^{-1} at concentrations ranging from 100 to 800 mg L^{-1}. The weighed amount of photocatalyst was ultrasonicated for 10 minutes in distilled water before being added to the feeding tank and magnetically stirred during the experiments. The pH was maintained at 6.8. Samples were taken at various time intervals throughout the process duration and enumerated using an agar dilution and streak plate procedure to determine the number of surviving bacteria in CFU mL^{-1} units.

To assess the effect of photocatalytic oxidation on conjugative gene transfer during the simultaneous exposure of both donor and recipient strains, a mixture of *E. coli* ATCC33694 recipient strain and *E. coli* DSM3876 donor strain in a 9:1 ratio was used [46]. The ten-fold excess was used to provide suitable conjugative pair formation conditions comparable to recent literature findings. The total number of enumerated transconjugants was expressed as a percentage against the total number obtained in the no-treatment reference conditions. One mL sample were taken along the PC process duration and subjected to the conjugative gene transfer assessment protocol.

3 Results and discussion

3.1 Material characterization

Mainly the characterization results are briefly summarized with refer to the previous study comparing different NCs regarding their photocatalytic activities and bacteria inactivation potentials [44]. The physical attributes of a sample can be characterized by its morphology, which describes its surface area structure. The CFT-GO nanocomposite exhibits a mesoporous structure with a narrow distribution of pore sizes, affording high adsorption capacities (35.2 m^2 g^{-1} BET, 390 m^2 g^{-1} Langmuir) [44].

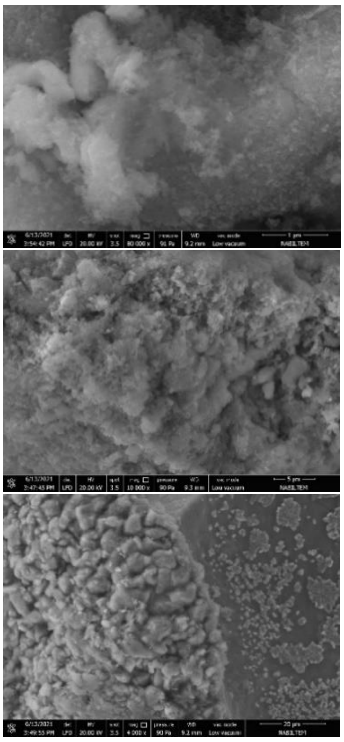

Figure 2. SEM analysis results of CFT-GO 3% nanocomposite

Nitrogen adsorption-desorption measurements revealed an average pore size of 13.9 µm. Additionally, the grain size was determined to be 75 nm based on XRD analysis and the application of the Scherrer equation, as it was recently reported [44].

The diffuse reflectance analysis was employed to evaluate the reduced band gap of CFT-GO. The role of free excitation energy of the bandgap on the bacteria inactivation potential of graphene-oxide supported nanocomposites was examined using photoluminescence analysis. The visible light absorption shifts resulting from the addition of graphene-oxide into the nanocomposite were analyzed with the help of Diffuse reflectance analysis. A previous study presented a comprehensive description of the characterization results [44].

3.2 *Bacteria inactivation kinetics – determining the sub-lethal photocatalysis conditions)*

In the experimental conditions investigated, the photo-catalytic (PC) process under continuous mode of operation using CFT-GO (carbon felt supported titanium dioxide-graphene oxide) photocatalyst was capable of maintaining sub-lethal conditions for 180 minutes at an initial concentration of 200 mg L^{-1} (Figure 3). Upon exposure to UV-vis irradiation, a significant level of inactivation (2 logarithmic reduction) was achieved, with the inactivation profile being evenly distributed throughout the process and not featuring any distinct logarithmic reduction phase [23,49]. It was found that at higher doses of 600 and 800 mg L^{-1}, the CFT-GO-based UV-vis driven photocatalysis resulted in removal rates of >5 logarithms. A comparison with the relevant literature revealed that a >4 logarithmic reduction was reported in a CPC flow-through reactor and that an optimum TiO_2 concentration of 0.200 g L^{-1} was identified for efficient bacteria inactivation in a CPC system. During the re-circulating continuous mode of operation, the initial delay (that is represented by the shoulder behavior) in the inactivation profile gradually decreases with increasing PC dose (Figure 3).

During the re-circulating continuous mode of operation, the initial delay in the inactivation profile, as represented by the shoulder behavior, gradually diminishes with an increase in the PC dose (as shown in Figure 3). At higher initial concentrations of PC, the logarithmic phase of inactivation becomes evident, and the inactivation rates gradually increase over time, similar to the findings reported with Mn-doped TiO_2 photocatalyst in a batch reactor and TiO_2 photocatalysts in a flow-through CPC reactor (as reported in [50,51]. Several studies have demonstrated that for high PC concentrations, the efficiency of the process decreases due to the shielding effect that inhibits ROS formation [52]. However, this effect is considerably less pronounced in the continuous re-circulating mode of operation. Theoretically, in this mode of operation, the liquid is fed into the reactor as a thin layer, with the photocatalyst and bacteria homogeneously mixed within the liquid that flows down through the inner wall of the reactor. The liquid layer is directly exposed to UV irradiation, and the photocatalysis process is carried out more efficiently. Reproducible individual PC bacteria inactivation rates were obtained for donor, recipient, and mated (transconjugant) strains (as shown in Figure 5).

3.3 *Effect of photocatalyst type and the mode of operation on bacteria inactivation kinetics*

A comparative evaluation of PC bacteria inactivation by CFT-GO and TiO_2 under two different modes of operation was carried out. The hole oxidation mechanism on the CFT-GO surface adsorbed cells may have resulted in a higher level of bacterial inactivation compared to TiO_2-UV-A based photocatalysis. However, in batch mode, the solution becomes opaque as a result of the heterogeneous photocatalysis conditions where the photocatalyst and the reactants are in seperated phases. As a result, UV irradiation can not effectively penetrate through the liquid, which may hinder the PC process rates. The shielding effect is more apparent under these conditions. Real wastewater matrixes might require higher UV energy due to absorption and shielding of UV-energy by naturally occurring wastewater constituents and photocatalysts [29,53].

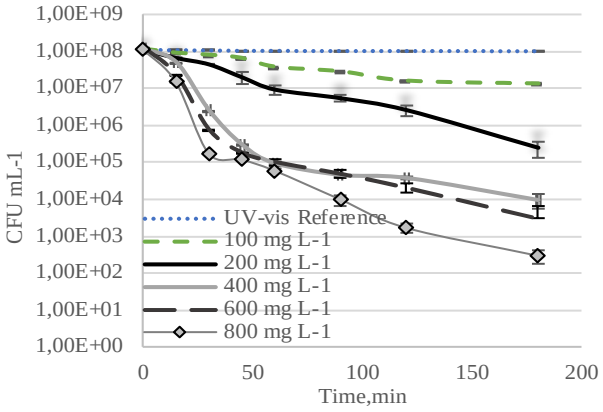

Figure 3. Effect of initial CFT-GO PC concentration on bacteria inactivation rates $[C]_{0\ bacteria}$: 10^8 CFU mL^{-1}

A continuous re-circulating mode of operation has advantages such as overcoming UV energy limitations, resulting in simultaneous and more efficient photocatalyst activation, generation of ROS species, and bacteria inactivation mechanisms occurring in a unit volume of bacteria-photocatalyst suspension. TiO_2-UV-A based PC resulted in an initial delay and post delay in the bacteria inactivation profile that was more spread over time than UV-vis driven CFT-GO photocatalysis, with a limited LOG inactivation phase, ending up with a total 1 LOG removal. On the other hand, CFT-GO based photocatalysis resulted in 2 LOGs of removal, with the bacteria inactivation profile in batch mode being more subject to initial delays and spread over time, with inactivation rates reaching a maximum of 1.5 LOG for both TiO_2-UV-A and CFT-GO-UV visible driven photocatalysis (Figure 4). The findings are comparable with those obtained for sub-lethal oxidative conditions provided by UV-vis driven 50 mg L^{-1} nano sphalerite and UV365 nm driven TiO_2 of 100 mg L^{-1} photocatalysis [23,49]. According to literature comparison, there were no variations regarding

bacterial strain resistance to photocatalytic induced oxidative stress conditions between acquired resistance of laboratory strains or natural strains from the same type carrying different ARGs [54,55].

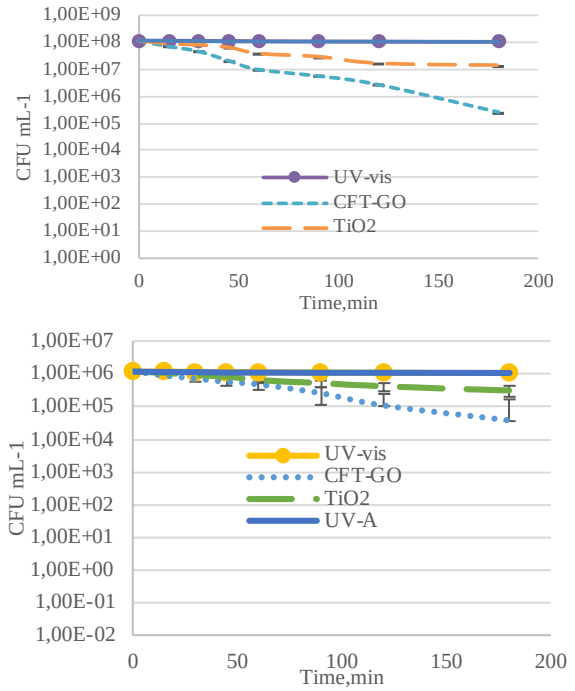

Figure 4. Rate of photocatalytic bacteria inactivation with CFT-GO, and TiO2 photocatalysts and at reference conditions a) Continuous and b) Batch mode of operation pH: 6.8, C]PC = 0.200 g L-1

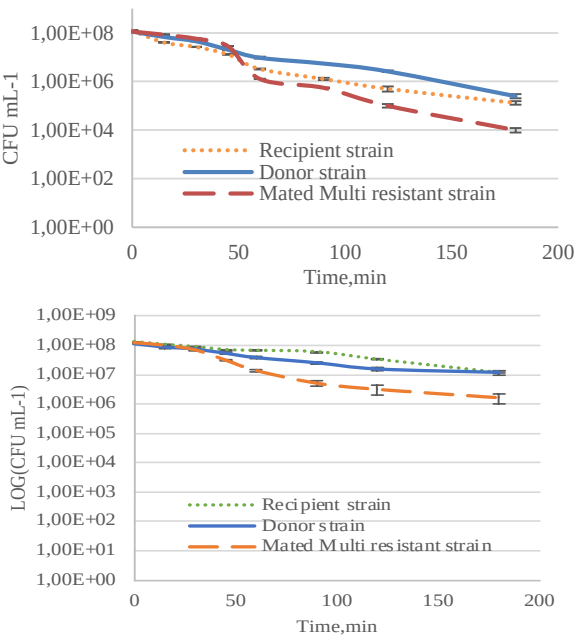

Figure 5. PC bacteria inactivation profiles of individual bacterial strains under a) UV-vis driven CFT-GO photocatalysis and b) UV-A driven TiO2 photocatalysts, at continuous mode of operation, pH: 6.8, [C]PC = 0.200 g L-1

3.4 *Effect of photocatalyst type and the mode of operation on bacteria inactivation kinetics*

The present study aimed to investigate the potential of *E.coli* DSM 3876 and *E.coli* ATCC33694 strains for RP4 plasmid-mediated conjugative gene transfer, based on preliminary experiments. The results indicated that successful gene transfer occurred between the two strains. To determine the optimal mating duration, the number of trans-conjugants formed was assessed at various time points. The findings showed that a mating duration of 20 hours yielded the highest number of trans-conjugants, which is consistent with previous studies. Consequently, a total mating duration of 20 hours was adopted for the subsequent evaluation of conjugative transfer (Figure 6) [49].

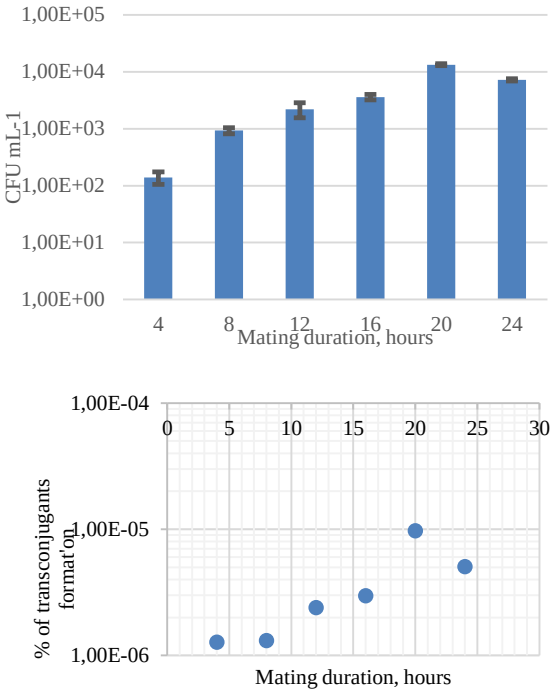

Figure 6. Effect of mating time on the conjugative transfer from *E. coli* DSM3876 (donor strain) to *E. coli* ATCC33694 (recipient strain). Donor: Recipient ratio set as 1:1, [C]0= 108 CFU mL-1.

In the absence of a limiting factor for recipient cells during conjugation, the availability of donor cells was increased by inducing cell permeability through the generation of intracellular reactive oxygen species (ROS). When intact recipient cells were exposed to photocatalytic (PC) oxidation before mating with donor cells, both the frequency and the number of transconjugants increased up to 60 minutes of process duration, after which they remained stable and followed a decreasing trend (as illustrated in Figure 7). Conversely, when recipient cells were mated with intact donor cells, the frequency of conjugative transfer increased following 90 minutes of photocatalysis process duration. The total number of transconjugants initially increased sharply, then declined and eventually stabilized at 1-2 x 10^2 CFU mL^{-1}. Unlike previous findings in the literature, the decline in conjugative transfer cannot be

attributed solely to loss of bacterial viability. The PC-mediated bacterial inactivation was carried out under sub-lethal conditions, allowing for continuous stress response in bacteria during the process duration [38,49]. Literature suggests that recipient-induced scenarios play a more significant role in assessing changes in the conjugative gene transfer caused by the applied treatment processes. Accordingly, as shown in Figure 7, both the frequency and absolute abundance of trans-conjugants following the PC process in continuous mode of operation remained significantly lower than the values obtained in batch mode of operation [22,23,38].

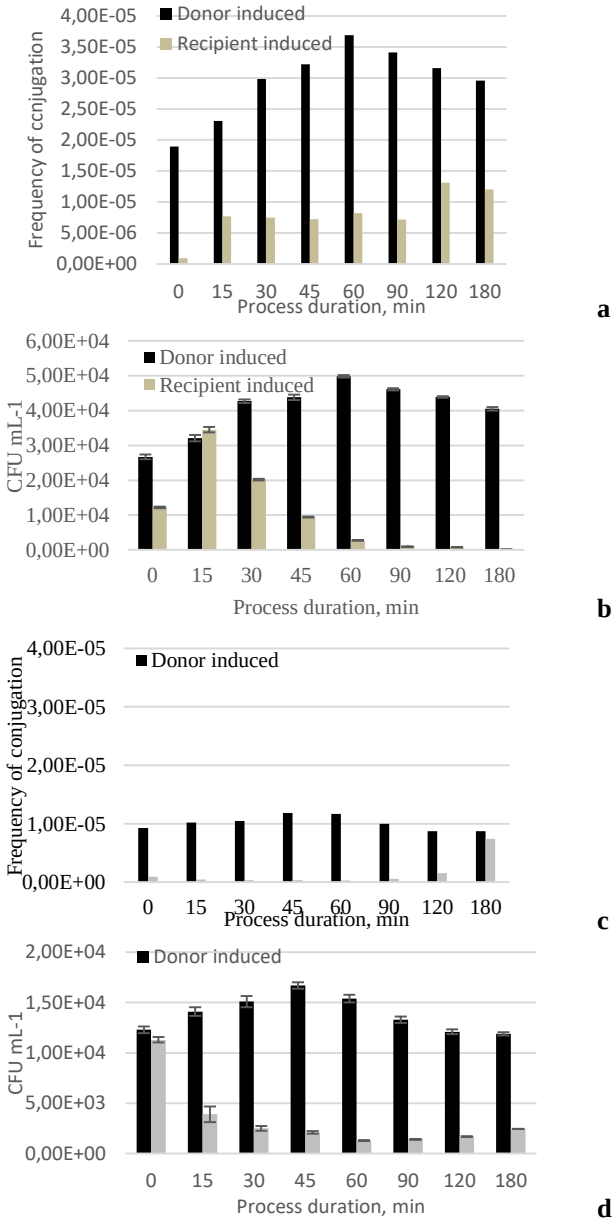

Figure 7. Effect of CFT-GO UV-vis PC induced donor and recipient strains on the a-c) conjugative transfer frequencies and b-d) total number of transconjugants formation. UV-vis: 3.30 mw cm^2, pH: 6.8, $[C]_{PC}$= 0.200 g L^{-1} under(a-b) continuous re-circulating – c,d) batch modes of operation.

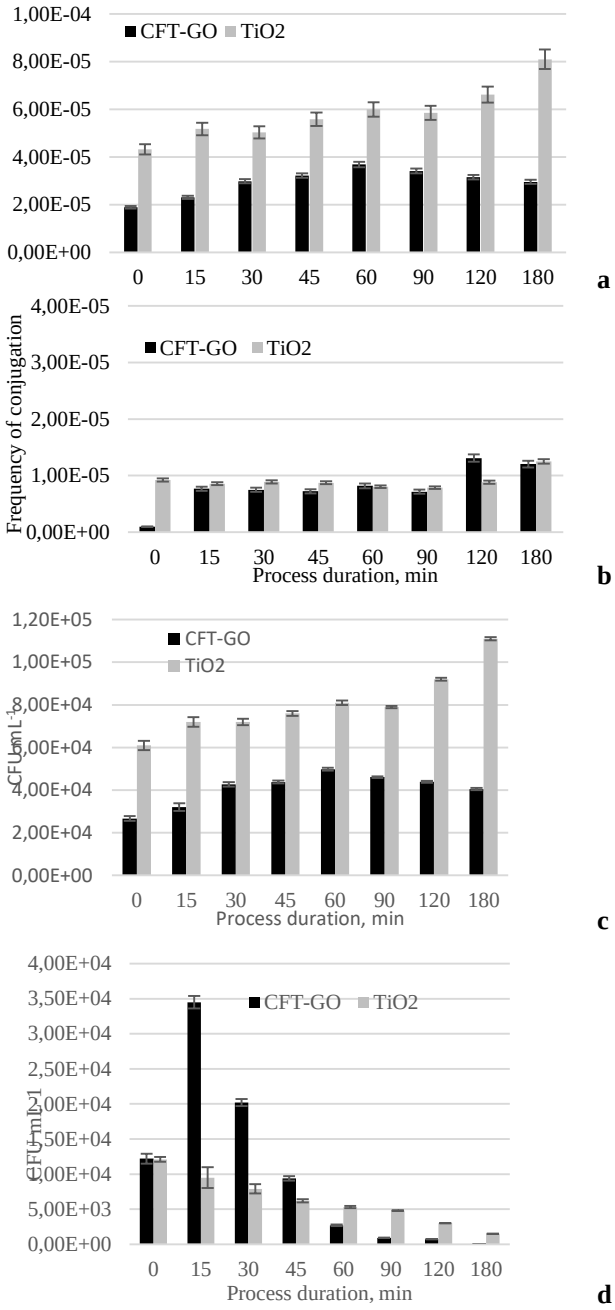

Figure 8. Effect of CFT-GO UV-vis and TiO_2-UV-A based photocatalytic oxidation on the conjugative transfer frequencies, and the number of trans-conjugants formation (notated as a-c: donor induced, b-d: recipient induced. UV-A irradiation: 2.20 mw cm^{-1}, UV-vis: 3.30 mw cm^{-1}, pH: 6.8, $[C]_{PC}$= 0.200 g L^{-1}under continuous re-circulating mode of operation.

In the comparative analysis of the impact of two photocatalysts on conjugative transfer, it was observed that the inhibition effect of TiO_2-based UV-A driven photocatalytic oxidation was limited in comparison to that of CFT-GO nanocomposite. The observed difference could be attributed to the differences in the extent and nature of

bacterial cell damage mechanisms induced by the two photocatalysts, as depicted in Figure 8.

Comparing, photocatalytic oxidation mechanism of two photocatalysts on the donor bacteria; exposure to a lower concentration of reactive oxygen species (ROS), and limited level of surface interactions between the photocatalyst and bacterial cells may bring along the differences observed with use of TiO_2. However, in the case of CFT-GO nanocomposite, the hydrophobic-hydrophilic transition of UV-irradiated graphene oxide may have enhanced the adhesion and facilitated the effect of hole oxidation mechanism on surface-adsorbed bacterial cells, also including cells in suspension form. The surface properties, dominant ROS formation, and bacterial cell oxidation pathways of highly porous reduced graphene-oxide foams in the presence of peroxymonosulfate were discussed in detail in a previous study [56], where the partial restoration of p-p conjugation within graphene sheets was also discussed. The study reported that the CFT-GO nanocomposite had graphite layer defects, including C disorders [44].

Previous research has reported similar results in utilizing photocatalytic inactivation techniques with TiO_2&Ag nanocomposites incorporating graphene-oxide, which have demonstrated limited effects on promoting antibiotic resistance gene (ARG) transfer [42]. More recent investigations have shown that highly porous reduced graphene-oxide with improved adsorptive and photocatalytic properties can enhance the photocatalytic treatment of antibiotic-resistant bacteria (ARB) and control ARG dissemination properties [29,42,57,58]. Additionally, another study proposed that the transfer of graphene-oxide-mediated ARGs could be affected by the reduction pathway of the nanomaterial [39].

When both donor and recipient strains are exposed to photocatalytic oxidation simultaneously, it leads to variations in both the rates of inactivation and formation of trans-conjugants compared to untreated conditions (Figure 9a, 9b). This is due to sub-lethal oxidative stress induced by photocatalytic oxidation, which enhances the transfer of antibiotic resistance genes (ARGs) during conjugation, while at the same time, the high adsorption capacity and adhesive surface interactions of CFT-GO with bacterial cells inhibit conjugation [2,26,59].

The incorporation of mesoporous CFT-GO nanocomposite and its high BET surface area exhibit advanced adhesive properties leading to increased rates of bacteria inactivation. Literature reports demonstrate that lower CFT nanocomposite doses result in higher photocatalytic activity, while the addition of varying doses of GO into the nanocomposite leads to increased bacteria inactivation rates (e.g. CFT-GO 3% and CFT-GO 1% exhibited higher rates of bacteria inactivation compared to TiO_2-based photocatalysis with k values of 3.43, 1.54, and 0.66, respectively, according to the HOM model) [44].

In this study, the adsorption capacity of the mesoporous CFT-GO nanocomposite limits the possibility of random pairings of donor and recipient strains in the aquatic environment, thereby limiting the increase in conjugative transfer. During the early stages (0-30 min) of PC treatment, the conjugative transfer is under adsorption limiting conditions and PC inactivation rates are high, while between 45-60 minutes, lower PC inactivation rates are observed and conjugative transfer is still limited due to the inhibiting effect of the CFT-GO nanocomposite photocatalyst. Between 90-120 minutes, high PC inactivation rates and possible desorption of adsorbed bacterial cells and extra-cellular genetic material result in the enhancement of conjugative transfer. At the end of 180 minutes, the percentage of mated pairs compared to the no-treatment conditions shows a significant decrease due to the depletion of recipient strains and a general reduction in the total number of bacteria cells ($CFU\ mL^{-1}$). Bacterial adsorption near photocatalytic sites not only favors efficient bacteria inactivation but also has the potential to promote the extracellular ARGs capturing and degradation mechanism. Thus, the GO-based photocatalyst may mitigate the HGT mechanism by transformation besides its physical barrier function between the surface-adsorbed donor and recipient strains. On the other hand, a delay in the onset of the gene pair conjugates was evident for the batch mode of operation (in accordance with the obtained PC bacteria inactivation rates) compared to the continuous mode (Figure 9).

Recent literature findings suggest that the increased affinity between bacteria and nitrogen-doped reduced graphene-oxide (NrGO) is attributed to the enhanced hydrophobic interactions between the photocatalyst surface and bacterial surface proteins [29]. The state of stress response and vitality of bacteria are critical factors in determining the conjugative transfer of antibiotic resistance genes (ARGs) [37]. During visible light-driven photocatalysis, prolonged exposure may increase the conjugative transfer rates due to long-term vitality of bacteria [38]. In a pioneering study, the transfer mechanisms of resistance genes between K12-susceptible and J53-rifampicin-resistant strains of *E. coli* bacterial cells (which were damaged but not completely inactivated under oxidative conditions created by the FK process) were investigated in distilled water and secondary treatment effluent environments. The study reports that the oxidative stress level of *E. coli* and the formation rate of conjugated gene pairs are reduced due to the reactive oxygen species (ROS) scavenging activity of the organic and inorganic components in the secondary treatment effluent, which is described as the mechanism of suppressing horizontal gene transfer (HGT) [46].

In this study, a maximum increase of 2.5-fold in the number of transconjugants was observed during photocatalytic oxidation, and this percentage remained below 1 by the end of the process duration, in comparison to the reference conditions where no treatment was applied (Figure 9). Since the study was conducted in a distilled water matrix, no ROS scavenger or favorable conditions for bacterial regrowth were present. The adhesion mechanism may have played a significant role in the interactions and contact between donor and recipient bacterial strains, preventing gene transfer channels and thus inhibiting the conjugative mechanism [34,39,42]. The unique lamellar structure and high adsorption properties of GOs could encase

bacterial cells and prevent the cell exchange mechanism with the external environment.

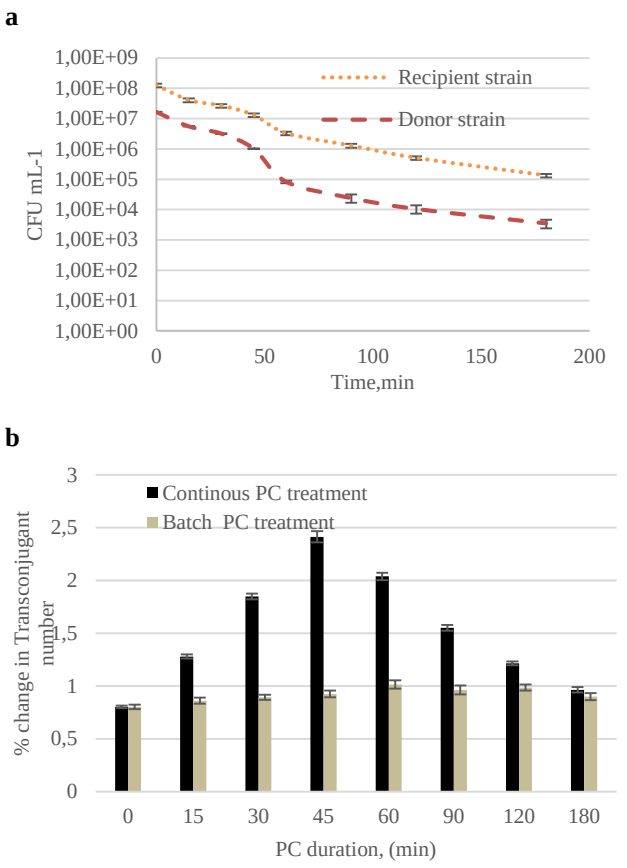

Figure 9. a) Bacteria inactivation and **b)** increase percentages of number of transconjugant strains during simultaneous exposure of donor and recipient strains to CFT-GO UV-vis PC under continuous mode of operation, Donor: Recipient ratio set as 9:1, $[C]_{0\ bacteria}$: 10^8 CFU mL^{-1}

4. Conclusion

The utilization of a UV-vis driven photocatalyst based on Graphene-oxide Ti-$CuFe_2O_4$ under sub-lethal photocatalytic conditions demonstrated enhanced bacterial inactivation and reduced conjugative gene transfer compared to reference UV-A TiO_2. For advanced oxidation processes to gain wider acceptance and be implemented at a larger scale, it is crucial to understand their impact on the mechanism of ARG propagation. The mode of process operation was observed to have a significant effect on the vitality of recipient cells, with the continuous mode of operation mitigating the transfer of ARGs and leading to a drastic decrease in the total number of cultivable bacteria cells following exposure to the CFT-GO based photocatalysis. However, it should be noted that the possibility of ARG exchange via natural transformation was not considered in this study, and further research is needed to simultaneously analyze both aspects of ARG transfer at the molecular scale. Experiments in natural water matrices and/or representative conditions have the utmost importance for large-scale applications to become widespread. In order to achieve effective bacterial inactivation and control of ARGs, it is recommended to consider the reactor configuration and operating regime in photocatalysis, in addition to the selection of the appropriate photocatalyst.

Acknowledgement

As the author of the study, I would like to acknowledge Prof. Dr. Ayten Yazgan Karataş from İstanbul Technical University, Department of Molecular Biology and Genetics and Prof. Dr. İdil Arslan Alaton from İstanbul Technical University, Department of Environmental Engineering for their support.

Data Availability

The datasets generated during and/or analyzed during the current study are available from the corresponding author upon reasonable request.

Funding

Authors would like to thank TNKU Scientific Research Projects Funding Office for the support within the research project NKUBAP.06.GA.21.343.

Conflict of interest

The authors declare that there is no conflict of interest.

Declaration of interests

The authors declare that they have no known competing financial interests or personal relationships that could have appeared to influence the work reported in this paper.

Similarity Rate: 15%.

References

[1] A. Catalano, D. Iacopetta, J. Ceramella, D. Scumaci, F. Giuzio, C. Saturnino, S. Aquaro, C. Rosano, M.S. Sinicropi, Multidrug Resistance (MDR): A widespread phenomenon in pharmacological therapies, Molecules, 27, 2022. doi:10.3390/molecules27030616.

[2] Y. Zhang, A.Z. Gu, M. He, D. Li, J. Chen, Subinhibitory concentrations of disinfectants promote the horizontal transfer of multidrug resistance genes within and across genera, Environ. Sci. Technol., 51, 570–580, 2017. doi:10.1021/acs.est.6b03132.

[3] I. Michael, L. Rizzo, C.S. McArdell, C.M. Manaia, C. Merlin, T. Schwartz, C. Dagot, D. Fatta-Kassinos, Urban wastewater treatment plants as hotspots for the release of antibiotics in the environment: A review, Water Res., 47, 957–995, 2013. doi:10.1016/j.watres.2012.11.027.

[4] C.B. Özkal, 11 Control of antibiotic resistance by advanced treatment: recent advances, in a nutshell, Environ. Microbiol. Emerg. Technol, 265, 2022.

[5] P.Y. Hong, T.R. Julian, M.L. Pype, S.C. Jiang, K.L. Nelson, D. Graham, A. Pruden, C.M. Manaia, Reusing treated wastewater: Consideration of the safety aspects associated with antibiotic-resistant bacteria and antibiotic resistance genes, Water, 10, 2018. doi:10.3390/w10030244.

[6] D.-W. Kim, C.-J. Cha, Antibiotic resistome from the One-Health perspective: understanding and controlling antimicrobial resistance transmission, Exp. Mol. Med., 53, 301-309, 2021.
[7] J. Davies, Inactivation of antibiotics and the dissemination of resistance genes, Science, 264, 375–382, 1994.
[8] R. Jayaraman, Antibiotic resistance: an overview of mechanisms and a paradigm shift, Curr. Sci., 1475–1484, 2009.
[9] M.P. Nikolich, G. Hong, N.B. Shoemaker, A.A. Salyers, Evidence for natural horizontal transfer of tetQ between bacteria that normally colonize humans and bacteria that normally colonize livestock., Appl. Environ. Microbiol., 60, 3255–3260, 1994.
[10] A. Goulas, B. Livoreil, N. Grall, P. Benoit, C. Couderc-Obert, C. Dagot, D. Patureau, F. Petit, C. Laouénan, A. Andremont, What are the effective solutions to control the dissemination of antibiotic resistance in the environment? A systematic review protocol, Environ. Evid. 7, 1–9, 2018. doi:10.1186/s13750-018-0118-2.
[11] F. Barancheshme, M. Munir, Strategies to combat antibiotic resistance in the wastewater treatment plants, Front. Microbiol. 8, 2018. doi:10.3389/fmicb.2017.02603.
[12] E. Jamrozik, M. Selgelid, Ethics and drug resistance: collective responsibility for global public health, 2020.
[13] K. Liguori, I. Keenum, B.C. Davis, J. Calarco, E. Milligan, V.J. Harwood, A. Pruden, Antimicrobial resistance monitoring of water environments: A framework for standardized methods and quality control, Environ. Sci. Technol. 56, 9149–9160, 2022.
[14] C.U. Schwermer, P. Krzeminski, A.C. Wennberg, C. Vogelsang, W. Uhl, Removal of antibiotic resistant *E. coli* in two Norwegian wastewater treatment plants and by nano- and ultra-filtration processes, Water Sci. Technol. 77, 1115–1126, 2018. doi:10.2166/wst.2017.642.
[15] G. Ferro, F. Guarino, A. Cicatelli, L. Rizzo, β-lactams resistance gene quantification in an antibiotic resistant Escherichia coli water suspension treated by advanced oxidation with UV/H_2O_2, J. Hazard. Mater. 323 426–433, 2017. doi:10.1016/j.jhazmat.2016.03.014.
[16] M. Jin, L. Liu, D. Wang, D. Yang, W. Liu, J. Yin, Z. Yang, H. Wang, Z. Qiu, Z. Shen, Chlorine disinfection promotes the exchange of antibiotic resistance genes across bacterial genera by natural transformation, ISME J. 14, 1847–1856, 2020. doi: 10.1038/s41396-020-0656-9
[17] J. Lu, Y. Wang, M. Jin, Z. Yuan, P. Bond, J. Guo, Both silver ions and silver nanoparticles facilitate the horizontal transfer of plasmid-mediated antibiotic resistance genes, Water Res., 169, 2020. doi:10.1016/j.watres.2019.115229.
[18] Z. Qiu, Z. Shen, D. Qian, M. Jin, D. Yang, J. Wang, B. Zhang, Z. Yang, Z. Chen, X. Wang, C. Ding, D. Wang, J.W. Li, Effects of nano-TiO_2 on antibiotic resistance transfer mediated by RP4 plasmid, Nanotoxicology. 9, 895–904, 2015. doi:10.3109/17435390.2014.991429.
[19] S. Zhang, Y. Wang, H. Song, J. Lu, Z. Yuan, J. Guo, Copper nanoparticles and copper ions promote horizontal transfer of plasmid-mediated multi-antibiotic resistance genes across bacterial genera, Environ. Int. 129, 478–487, 2019. doi:10.1016/j.envint.2019.05.054.
[20] S. Ghosh, Y. Chen, J. Hu, Application of UVC and UVC based advanced disinfection technologies for the inactivation of antibiotic resistance genes and elimination of horizontal gene transfer activities: Opportunities and challenges, Chem. Eng. J. 450, 2022. doi:10.1016/j.cej.2022.138234.
[21] C. Kong, X. He, M. Guo, S. Ma, B. Xu, Y. Tang, The Impacts of Chlorine and Disinfection Byproducts on Antibiotic-Resistant Bacteria (ARB) and Their Conjugative Transfer, Water, 14, 2022. doi:10.3390/w14193009.
[22] X. Chen, H. Yin, G. Li, W. Wang, P.K. Wong, H. Zhao, T. An, Antibiotic-resistance gene transfer in antibiotic-resistance bacteria under different light irradiation: Implications from oxidative stress and gene expression, Water Res. 149, 282–291, 2022. doi:10.1016/j.watres.2018.11.019.
[23] H. Ji, Y. Cai, Z. Wang, G. Li, T. An, Sub-lethal photocatalysis promotes horizontal transfer of antibiotic resistance genes by conjugation and transformability, Water Res., 221, 2022. doi:10.1016/j.watres.2022.118808.
[24] R.K. Manoharan, F. Ishaque, Y.H. Ahn, Fate of antibiotic resistant genes in wastewater environments and treatment strategies - A review, Chemosphere., 298, 2022. doi:10.1016/j.chemosphere.2022.134671.
[25] M.C. Maria, R.P. d. Mendonça Neto, G.F.F. Pires, P.B. Vilela, C.C. Amorim, Combat of antimicrobial resistance in municipal wastewater treatment plant effluent via solar advanced oxidation processes: Achievements and perspectives, Sci. Total Environ. 786, 2021. doi:10.1016/j.scitotenv.2021.147448.
[26] I. Michael-Kordatou, P. Karaolia, D. Fatta-Kassinos, The role of operating parameters and oxidative damage mechanisms of advanced chemical oxidation processes in the combat against antibiotic-resistant bacteria and resistance genes present in urban wastewater, Water Res. 129, 208–230, 2018. doi.org/10.1016/j.watres.2017.10.007
[27] G. Mamba, A. Mishra, Advances in magnetically separable photocatalysts: Smart, recyclable materials for water pollution mitigation, Catalysts, 2016. doi:10.3390/catal6060079.
[28] N.R. Khalid, A. Majid, M.B. Tahir, N.A. Niaz, S. Khalid, Carbonaceous-TiO_2 nanomaterials for photocatalytic degradation of pollutants: A review, Ceram. Int. 43, 14552–14571, 2022. doi.org/10.1016/j.ceramint.2017.08.143
[29] D. Li, P. Yu, X. Zhou, J.H. Kim, Y. Zhang, P.J.J. Alvarez, Hierarchical $Bi_2O_2CO_3$ wrapped with modified graphene oxide for adsorption-enhanced photocatalytic inactivation of antibiotic resistant

bacteria and resistance genes, Water Res., 184, 2020. doi:10.1016/j.watres.2020.116157.

[30] H. Wang, X. Li, Q. Ge, Y. Chong, Y. Zhang, A multifunctional Fe_2O_3@MoS_2@SDS z-scheme nanocomposite: NIR enhanced bacterial inactivation, degradation antibiotics and inhibiting ARGs dissemination, Colloids Surfaces B Biointerfaces., 219, 2022. doi:10.1016/j.colsurfb.2022.112833.

[31] K.K. Kefeni, B.B. Mamba, Photocatalytic application of spinel ferrite nanoparticles and nanocomposites in wastewater treatment: Review, Sustain. Mater. Technol. 23, 2020. e00140. doi:10.1016/j.susmat.2019.e00140.

[32] R. Kodasma, B. Palas, G. Ersöz, S. Atalay, Photocatalytic activity of copper ferrite graphene oxide particles for an efficient catalytic degradation of Reactive Black 5 in water, Ceram. Int., 46, 6284–6292, 2020. doi:10.1016/j.ceramint.2019.11.100.

[33] Q. Jiang, M. Feng, C. Ye, X. Yu, Effects and relevant mechanisms of non-antibiotic factors on the horizontal transfer of antibiotic resistance genes in water environments: A review, Sci. Total Environ., 806, 2022. doi:10.1016/j.scitotenv.2021.150568.

[34] P. Karaolia, I. Michael-Kordatou, E. Hapeshi, C. Drosou, Y. Bertakis, D. Christofilos, G.S. Armatas, L. Sygellou, T. Schwartz, N.P. Xekoukoulotakis, Removal of antibiotics, antibiotic-resistant bacteria and their associated genes by graphene-based TiO_2 composite photocatalysts under solar radiation in urban wastewaters, Appl. Catal. B Environ., 224, 810–824, 2018. doi.org/10.1016/j.apcatb.2017.11.020

[35] K. Yu, F. Chen, L. Yue, Y. Luo, Z. Wang, B. Xing, CeO_2 nanoparticles regulate the propagation of antibiotic resistance genes by altering cellular contact and plasmid transfer, Environ. Sci. Technol. 54, 10012-10021, 2020. doi.org/10.1021/acs.est.0c01870

[36] L. Shi, J. Chen, L. Teng, L. Wang, G. Zhu, S. Liu, Z. Luo, X. Shi, Y. Wang, L. Ren, The antibacterial applications of graphene and its derivatives, Small. 12, 4165–4184, 810–824, 2022. doi:10.1002/smll.201601841.

[37] D. Xia, H. Liu, Z. Jiang, T.W. Ng, W.S. Lai, T. An, W. Wang, P.K. Wong, Visible-light-driven photocatalytic inactivation of *Escherichia coli* K-12 over thermal treated natural magnetic sphalerite: Band structure analysis and toxicity evaluation, Appl. Catal. B Environ. 224, 541–552, 2018. doi.org/10.1016/j.apcatb.2017.10.030

[38] H. Yin, X. Chen, G. Li, W. Wang, P.K. Wong, T. An, Can photocatalytic technology facilitate conjugative transfer of ARGs in bacteria at the interface of natural sphalerite under different light irradiation, Appl. Catal. B Environ., 287, 2021. doi:10.1016/j.apcatb.2021.119977.

[39] Q. Zhang, X. Liu, H. Zhou, Y. Lu, Y. Fan, L. Wu, X. Xiao, Reduction pathway of graphene oxide affects conjugation-mediated horizontal gene transfer under environmental conditions, Chem. Eng. J. 450, 2022. doi:10.1016/j.cej.2022.138301.

[40] M.A.S. Mc Mahon, I.S. Blair, J.E. Moore, D.A. Mc Dowell, The rate of horizontal transmission of antibiotic resistance plasmids is increased in food preservation-stressed bacteria, J. Appl. Microbiol. 103, 1883–1888, 2007. doi:10.1111/j.1365-2672.2007.03412.x.

[41] C.A. Woodall, E . coli Plasmid Vectors DNA Transfer by Bacterial Conjugation, Methods Mol. Biol., 235, 61–65, 2003. doi.org/10.1385/1-59259-409-3:61

[42] M.T. Guo, X.B. Tian, Impacts on antibiotic-resistant bacteria and their horizontal gene transfer by graphene-based TiO_2&Ag composite photocatalysts under solar irradiation, J. Hazard. Mater., 380, 2019. doi:10.1016/j.jhazmat.2019.120877.

[43] C.B. Ozkal, S. Meric, Photocatalytic Bacteria Inactivation by TiO_2-Ag based Photocatalysts and the Effect on Antibiotic Resistance Profile, Curr. Anal. Chem., 17, 98–106, 2021. doi.org/10.2174/1573411016999200711145845

[44] C.B. Özkal, Synthesis of $CuFe_2O_4$-Ti and $CuFe_2O_4$-Ti-GO nanocomposite photocatalysts using green-synthesized $CuFe_2O_4$: determination of photocatalytic activity, bacteria inactivation and antibiotic degradation potentials under visible light, J. Chem. Technol. Biotechnol., 97(7), 1842-1859, 2022. doi.org/10.1002/jctb.7058

[45] I.A. Alaton, A.Y. Karataş, Ö. Pehlivan, T.O. Hanci, Elimination of antibiotic resistance in treated urban wastewater by iron-based advanced oxidation processes, Desalin. Water Treat., 172, 235–253, 2019. doi:10.5004/dwt.2019.24929.

[46] P.S.M. Dunlop, M. Ciavola, L. Rizzo, D.A. McDowell, J.A. Byrne, Effect of photocatalysis on the transfer of antibiotic resistance genes in urban wastewater, Catal. Today., 240, 55–60, 2015. doi:10.1016/j.cattod.2014.03.049.

[47] D. Saha, M.C. Visconti, M.M. Desipio, R. Thorpe, Inactivation of antibiotic resistance gene by ternary nanocomposites of carbon nitride, reduced graphene oxide and iron oxide under visible light, Chem. Eng. J., 382, 2020. doi:10.1016/j.cej.2019.122857.

[48] H. Wang, J. Wang, S. Li, G. Ding, K. Wang, T. Zhuang, X. Huang, X. Wang, Synergistic effect of UV/chlorine in bacterial inactivation, resistance gene removal, and gene conjugative transfer blocking, Water Res., 185, 2020. doi:10.1016/j.watres.2020.116290.

[49] H. Yin, X. Chen, G. Li, Y. Chen, W. Wang, T. An, P.K. Wong, H. Zhao, Sub-lethal photocatalysis bactericidal technology cause longer persistence of antibiotic-resistance mutant and plasmid through the mechanism of reduced fitness cost, Appl. Catal. B Environ., 245, 698–705, 2019. doi.org/10.1016/j.apcatb.2019.01.041

[50] Venieri, D.; Fraggedaki, A.; Kostadima, M.; Chatzisymeon, E.; Binas, V.; Zachopoulos, A.; Kiriakidis, G.; Mantzavinos, D. Solar light and metal-doped TiO2 to eliminate water-transmitted bacterial pathogens: Photocatalyst characterization and disinfection performance. Appl Catal B 2014, 154, 93–101, doi:10.1016/j.apcatb.2014.02.007.

[51] Alrousan, D.M.A.; Dunlop, P.S.M.; McMurray, T.A.; Byrne, J.A. Photocatalytic inactivation of *E. coli* in surface water using immobilised nanoparticle TiO_2 films. Water Res 2009, 43, 47–54. doi.org/10.1016/j.watres.2008.10.015

[52] Mehrotra, K.; Yablonsky, G.S.; Ray, A.K. Kinetic Studies of photocatalytic degradation in a TiO_2 slurry system: Distinguishing working regimes and determining rate dependences. Ind Eng Chem Res 2003, 42, 2273–2281. doi.org/10.1021/ie0209881

[53] P. Fernández-Ibáñez, C. Sichel, M.I. Polo-López, M. de Cara-García, J.C. Tello, Photocatalytic disinfection of natural well water contaminated by Fusarium solani using TiO_2 slurry in solar CPC photo-reactors, Catal. Today., 144, 62–68, 2009. doi.org/10.1016/j.cattod.2009.01.039

[54] T. Tsai, H. Chang, K. Chang, Y. Liu, A comparative study of the bactericidal effect of photocatalytic oxidation by TiO_2 on antibiotic-resistant and antibiotic-sensitive, J. áChem. Technol. Biotechnol., 85.12, 1642–1653, 2010. doi:10.1002/jctb.2476.

[55] V.M. Sousa, C.M. Manaia, A. Mendes, O.C. Nunes, Photoinactivation of various antibiotic resistant strains of Escherichia coli using a paint coat, J. Photochem. Photobiol. A Chem., 251, 148–153, 2013. doi:10.1016/j.jphotochem.2012.10.027.

[56] M. Karbasi, F. Karimzadeh, K. Raeissi, S. Rtimi, J. Kiwi, S. Giannakis, C. Pulgarin, Insights into the photocatalytic bacterial inactivation by flower-like Bi_2WO_6 under solar or visible light, through in situ monitoring and determination of reactive oxygen species (ROS), Water, 12, 2020. doi:10.3390/W12041099.

[57] V. Palmieri, F. Bugli, M.C. Lauriola, M. Cacaci, R. Torelli, G. Ciasca, C. Conti, M. Sanguinetti, M. Papi, M. De Spirito, Bacteria meet graphene: modulation of graphene oxide nanosheet interaction with human pathogens for effective antimicrobial therapy, ACS Biomater. Sci. Eng., 3, 619–627, 2017. doi.org/10.1021/acsbiomaterials.6b00812

[58] T. Pulingam, K.L. Thong, M.E. Ali, J.N. Appaturi, I.J. Dinshaw, Z.Y. Ong, B.F. Leo, Graphene oxide exhibits differential mechanistic action towards Gram-positive and Gram-negative bacteria, Colloids Surfaces B Biointerfaces., 181, 6–15, 2019. doi.org/10.1016/j.colsurfb.2019.05.023

[59] P. Chen, X. Guo, S. Li, F. Li, A review of the bioelectrochemical system as an emerging versatile technology for reduction of antibiotic resistance genes, Environ. Int., 156, 106689, 2021. doi.org/10.1016/j.envint.2021.106689